Fragmentation of multiply charged simple metal clusters in liquid-drop stabilized jellium model

M. Payami

January 8, 2022

Center for Theoretical Physics and Mathematics, Atomic Energy Organization of Iran, P. O. Box 11365-8486, Tehran, Iran

Abstract

In this work, we have used the liquid-drop model in the context of stabilized jellium model, to study the stability of Z-ply charged metal clusters of different species against fragmentation. We have shown that on the one hand, singly ionized clusters are stable against any spontaneous fragmentation, and on the other hand, the most favored decay process for them is atomic evaporation. However, multiply charged clusters of sufficiently small sizes may undergo spontaneous decay via fission processes. Comparing the results for different species show that for fixed N, the lower electron density metal clusters can accommodate more excess charges before their Coulomb explosions. This comparison also shows that, for fixed Z, the atomic evaporation which is the most favored decay mechanism for sufficiently large clusters, takes place at lower Ns for lower electron density clusters.

1 Introduction

Study of the stability of charged metal clusters against fragmentation is important in nano-sized systems. In this work, we have studied the binary fragmentation of N-atom Z-ply charged \mathcal{M}_N^Z clusters in the framework of the liquid-drop [1] model (LDM) with stabilized [2] jellium model (SJM) coefficients for the energies. Here, Z=1, 2, 3, 4; and \mathcal{M} covers the species Al, Ga, Li, Na, K, and Cs. Here, in the case of Al, when N is a multiple of 3, it corresponds to real Al $_{\nu}$ cluster with $\nu = N/3$. The clusters are assumed to be spherical with sizes determined by $R = N^{1/3} r_s^B$ with $N \leq 100$. The quantity r_s^B is the Wigner-Seitz radius of the electrons in the bulk metal. The possible decay channels of \mathcal{M}_N^Z are

$$\mathcal{M}_N^Z \to \mathcal{M}_{N-p}^{Z-Z_1} + \mathcal{M}_p^{Z_1} \tag{1}$$

Here, p is positive integer as N, and $0 \le Z_1 \le [Z/2]$. Different processes are defined by different values of Z_1 . The process in which $Z_1 = 0$ (one of the fragments is neutral), is called evaporation. The processes in which $0 < Z_1 = Z/2$ are called charge-symmetric fission, and the charge-asymmetric fission is defined by $0 < Z_1 < [Z/2]$. For any given set of values N, Z, Z_1 , different values of p define different decay channels. In a particular decay channel of the evaporation processes, the negativity of the difference between total energies before and after the fragmentation,

$$D^{Z}(N,p) = E^{Z}(N-p) + E^{0}(p) - E^{Z}(N),$$
(2)

is sufficient for the decaying in that particular channel. In the above equation, $E^Z(N)$ and $E^0(N)$ are the total energies of Z-ply ionized and neutral N-atom clusters, respectively. However, in fission processes a negative value for the difference energy is not a sufficient condition for the decay of the parent cluster. This is because, the competition between the short-range surface tension and the long-range repulsive Coulomb force may give rise to a fission barrier. The heights of the fission barriers are calculated using the two-spheres approximation[3]. In Fig. 1, the fission of a Z-ply charged N-atom cluster into two clusters of respective sizes N_1 , $N_2 = N - N_1$ and respective charges Z_1 , $Z_2 = Z - Z_1$ is schematically shown. Q_f is the energy release, B_c is the fusion barrier (or Coulomb barrier) which is the maximum energy of the Coulomb interaction of two positively-charged conducting spheres, taking their polarizabilities into account. B_f is the fission barrier height which is defined as

$$B_f = -Q_f + B_c. (3)$$

The Coulomb interaction energy, E_c , as a function of their separations, d, for two charged metallic spheres can be numerically calculated using the classical method of image charges [3].

The most favored decay channel in evaporation processes is defined as the channel for which the dissociation energy assumes its minimum value

$$D^{Z}(N, p^*) = \min_{p} \left\{ D^{Z}(N, p) \right\}, \tag{4}$$

and the most favored decay channel in fission processes is defined as the channel for which the fission-barrier height assumes its minimum value,

$$B_f(N, p^*) = \min_{p} \{B_f(N, p)\}.$$
 (5)

The energy of an N-atom Z-ply charged cluster in the LDM is given [4, 5] by

$$E^{Z}(N) = E^{0}(N) + Z(W + \frac{c}{R}) + \frac{Z^{2}e^{2}}{2(R+a)},$$
(6)

in which W, c, R, and e are the work function of the bulk metal, the finite-size correction to the work function, the radius of the cluster, and the electron charge, respectively. For simplicity, the position of the centroid of excess charge, a, is neglected in our calculations. $E^0(N)$ is the energy of a neutral N-atom cluster in the LDM, which is given by

$$E^{0}(N) = \varepsilon N + 4\pi (r_{s}^{B})^{2} \sigma N^{2/3} + 2\pi r_{s}^{B} \gamma N^{1/3}.$$
 (7)

In Eq. (7), the quantities ε , σ , and γ are total energy per electron of the bulk, surface energy, and curvature energy, respectively. We have calculated the quantities c, W, σ , and γ by fitting to the self-consistent Kohn-Sham [6] results in the SJM for different r_s values [5]. However, ε is calculated using the SJM energy expression for the bulk system (Eq. (1) of Ref. [7]).

2 Results and discussion

Using the method of image charges, we have calculated the Coulomb interaction energy of two charged metallic spheres, taking their polarizabilities into account. The calculations show that the maximum of the interaction energy, B_c , is achieved for a separation $d_0 \ge R_1 + R_2$. Fig. 2(a) shows the Coulomb interaction energy of an N_1 -atom cluster with another N_2 -atom of respective excess charges $Z_1 = 3$ and $Z_2=1$. The radii of the clusters are calculated from $R = N^{1/3} r_s^B$, as in the SJM. In this figure, we have taken $r_s^B=2.07$

which correspond to bulk Al. When both N_1 and N_2 are multiples of 3, the results correspond to real Al clusters. The value at the maximum specifies the quantity B_c , and the position of the maximum, d_0 , is the separation between the centers of the two spheres. As is seen, for fixed values of charges, B_c is the highest when the sizes are equal. In Fig. 2(b), the situation is shown for equal charges $Z_1 = Z_2 = 2$. In this case, when the sizes are equal, B_c is maximum as before but here, $d_0 = R_1 + R_2$. An other feature shown in Fig. 2(c) is that, when both charges and sizes are asymmetric, B_c is higher if the smaller charge corresponds to the smaller cluster. In Fig. 2(d), we have compared the Coulomb interaction energies of two Al metallic spheres with respective sizes $N_1 = 2$ and $N_2 = 18$ for different charges. It is seen that keeping the sizes fixed but increasing the charge on any one of them, without changing the charge on the other one, increases the height of the maximum.

In our calculations we need the values of the Coulomb interaction energy at the maxima points, i.e., the B_c s. In Fig. 3(a), we have compared the B_c values for equally charged $Z_1 = Z_2 = 1$, Al metallic particles but with different radii $R_1 = 2.07 N_1^{1/3}$ and $R_2 = 2.07 N_2^{1/3}$. This figure shows that when both of the sizes are small, the barrier is higher than the case when at least one of them is larger. In Fig. 3(b), we have compared the B_c s for singly ionized pairs Al, Na, and Cs with different values of N_1 and N_2 . In the aluminum case, since the radii of the spheres are smaller than those of Na and so on, their polarizabilities are thereby smaller and thus the Al values lie above that of Na, and so on. Now, if the charge on one of the clusters is increased without changing that of the other one, the arrangement of the curves would not change but they shift upward according to Fig. 2(d).

In the energy calculations of Eq. (6) we use the results obtained for c and W in Ref. [5]. The values of ε are calculated using Eq. (1) of Ref. [7] for unpolarized case. σ and γ in Eq. (7) are obtained by fitting the results of the self-consistent solutions of the Kohn-Sham equations in the SJM for neutral clusters of sizes $N \leq 100$, and different r_s values. The values of r_s^B for Al, Ga, Li, Na, K, and Cs are 2.07, 2.19, 3.28, 3.99, 4.96, and 5.63, respectively. In Figs. 4(a)-(c) we have plotted the SJM values of ε , σ , and γ , as functions of r_s , respectively.

To show the variations of the dissociation energy, $D^{Z}(N,p)$, for different charging and different evaporation channels, we have plotted, in Figs. 5(a)-(b), the quantities $D^{1+}(N,p)$ and $D^{4+}(N,p)$, respectively, as functions of the neutral fragment size, p, for Li. As is seen in Fig. 5(a), for small p values $D^{1+}(N,p)$ has an increasing behavior, then after passing a maximum, it changes to a decreasing behavior, and finally, for large p values it increases again. This behavior has its roots in the trade off between the surface energy (the volume energy term does not change in the fragmentation process) and the last term of Eq. (6).

For small p, the surface area difference

$$\Delta S(R_1, R) = 4\pi \left[R_1^2 + (R^3 - R_1^3)^{2/3} - R^2 \right], \tag{8}$$

increases, and then for intermediate p values, it assumes a maximum, and finally decreases. The increasing behavior at the tail is because, with increasing p, the size of the singly ionized fragment decreases and hence, beyond a certain p value, the last term in Eq. (6) dominates the surface energy term. However, beyond a Z value for the parent cluster, the last term of the Eq. (6) dominates the surface energy term for smaller p values before $D^Z(N,p)$ reaches its maximum as in the case of Fig. 5(b). In fact, we have found that for Li_{70}^Z this transition takes place at a point $1.6 < Z_t < 1.7$. The value of Z_t depends on N. This dependence is clearly shown in Fig. 5(a) by the fact that $D^{1+}(20,p)$ and $D^{1+}(10,p)$ are increasing functions of p in the whole range.

The dissociation energy $D^{Z}(N,p)$ for small p/N takes the form

$$D^{Z}(N,p) \to 2\pi \gamma r_s p^{1/3} + 4\pi \sigma r_s^2 p^{2/3},$$
 (9)

which specifies the most favored channel in an evaporation process with $p^* = 1$. This means that, in evaporation processes, the parent charged cluster prefers to evaporate single atoms than larger neutral clusters. This fact is also numerically shown in Figs. 5(a)-(b). On the other hand, the positivity of $D^Z(N, p)$ in the whole range implies that the parent charged cluster is stable against any spontaneous evaporation.

In Fig. 6, we have plotted the most favored dissociation energies, $D^{Z}(N, p^{*})$, of Na clusters as functions of the parent size, N, for different Z values. The results show that for large enough clusters, the dissociation energy is independent of Z, which is consistent with Eq. (9). However, for small clusters, the dissociation energy increases with charge.

Figures 7(a)-(b) compares the most favored dissociation energies of different species for Z=1 and Z=4, respectively. It is seen that detachment of a single atom from a lower electron density cluster is easier, i.e., it needs less energy. Comparing these two figures also shows that, although the hierarchy is the same, the dissociation energies are shifted to higher energies as we go from Z=1 to Z=4.

Now, we consider the fission processes. We first consider the following two cases:

$$Ga_N^{4+} \to Ga_{N-p}^{2+} + Ga_p^{2+},$$
 (10)

$$Ga_N^{4+} \to Ga_{N-p}^{3+} + Ga_p^{1+}.$$
 (11)

Processes (10) and (11) describe charge-symmetric and charge-asymmetric fissions, respectively. In Figs. 8(a) and 8(b) we have plotted their respective fission barriers,

 $B_f^{Z,Z_1}(N,p)$, for $Z_1=2,1$ as functions of p, for different sizes of the parent. As is seen in both of these figures, there exists a minimum size for the parent, N_{min}^{Z,Z_1} , beyond which the fission barrier height is positive in all possible channels of that particular process. That is, the parent cluster \mathcal{M}_N^Z with $N \geq N_{min}^{Z,Z_1}$ is stable against any spontaneous fission via that particular process.

One of the significant differences in the charge-symmetric and charge-asymmetric fission is that [as seen in Figs. 8(a) and 8(b)], in the most favored channel, the products have more or less the same sizes in the former case; whereas, in the latter case the less charged fragment assumes quite smaller sizes. That is, the charge-symmetric fission proceeds mostly via mass-symmetric channel, and the charge-asymmetric fission does it via mass-asymmetric channel. In Fig. 8(c), we compare the most favored sizes, p^* , for the charge-symmetric and charge-asymmetric fission of Na_N⁴⁺. It is seen that in the charge-symmetric case, p^* increases with N whereas, in the charge-asymmetric case it remains more or less constant.

To decide whether a cluster with a given size and charge, \mathcal{M}_N^Z , is stable against any spontaneous decay, one should compare N with the quantity

$$N_{min}^{Z} = \max_{Z_1} \left\{ N_{min}^{Z, Z_1} \right\}. \tag{12}$$

If $N \geq N_{min}^Z$, then the cluster \mathcal{M}_N^Z is stable against any spontaneous decay. To show the values of N_{min}^{Z,Z_1} schematically, we plot the most favored fission barriers, $B_f^{Z,Z_1}(N,p^*)$ for all possible Z_1 values. The evaporation processes need not be considered because, as was shown before, in the LDM there is no spontaneous decay via evaporation. However, in order to determine at what size which process is dominant, we include the most favored evaporation process as well. It should be mentioned that, in the self-consistent Kohn-Sham results [8], because of the shell effects, the spontaneous evaporation is also possible.

In Fig. 9, we have compared the most favored fission barriers, $B_f^{4,Z_1}(N,p^*)$, of Ga_N^{4+} for $N \leq 150$ and $Z_1 = 1,2$ with the most favored dissociation energy, $D^4(N,p^*)$. We have labeled the intersection points of the curves with each other and with the horizontal N axis by A, B, C, D, and E. At point A, the charge-symmetric and charge-asymmetric fission start their competition; thus we name the corresponding size as N_{s-a} . For clusters \mathcal{M}_N^{4+} with $N < N_{s-a}$, the charge-symmetric fission is dominant whereas for larger sizes charge-asymmetric one dominates. We name the size corresponding to the point B as $N_{min}^{4,2}$ because for sizes greater than this there is no charge-symmetric spontaneous fission. However, spontaneous fission via charge-asymmetric process still persists for $N_{min}^{4,2} < N < N_{min}^{4,1}$. Beyond the size $N_{min}^{4,1}$ which corresponds to the point C, the spontaneous charge-asymmetric fission also stops. Our results show that, for small r_s values, $N_{min}^{4,2} \leq N_{min}^{4,1}$ whereas, for $r_s > 4.5$, the reverse inequality is at work (as in the cases of K and Cs).

According to Eq. (12), if $N > N_{min}^Z$, then any spontaneous fission stops and the cluster \mathcal{M}_N^{4+} would be stable against any spontaneous decay. At sizes $N_{eva}^{4,2}$ and $N_{eva}^{4,1}$ which correspond, respectively, to the points D and E, competition of the evaporation with charge-symmetric and charge-asymmetric fission starts, respectively. Beyond the size

$$N_{eva}^{Z} = \max_{Z_1} \left\{ N_{eva}^{Z, Z_1} \right\}, \tag{13}$$

the dominant decay process is evaporation. Our results show that, at least for $r_s \leq 7$, the inequality $N_{eva}^{4,2} < N_{eva}^{4,1}$ is satisfied. When Z = 3, the decay processes consist of evaporation and charge-asymmetric fission whereas, for Z = 2, the fission is a charge-symmetric one.

In Figs. 10(a) and (b), we compare the most favored fission barrier heights $B_f^{3,1}(N, p^*)$ and $B_f^{2,1}(N, p^*)$ for different species, respectively. The figures indicate that, for large enough clusters, the fission barriers are higher for higher electron density metals.

In Fig. 11(a), we compare the smallest stable sizes, N_{min}^{Z} for different species. Looking at the figure, one concludes that, for fixed N, the higher electron density metal clusters (say Al) has less capacity for charging than the lower density metal clusters (say Cs). This behavior is observed for all 1 < Z < 4.

To show the size beyond which evaporation dominates all decay processes, we plot N_{eva}^Z with Z=2,3,4 for all species in Fig. 11(b). It is seen that, for fixed charge, Z, the evaporation process dominates at smaller N values for lower electron density metal clusters. The trends in Figs. 11(a) and 11(b) are seen to be the same.

Finally, in Fig. 11(c), we compare the N_{s-a} , the size at which the competition between the charge-symmetric and charge-asymmetric fission starts. This size decreases from Al to Li, and then increases from Li to K, and finally decreases from K to Cs. In the plot, we have taken into account the decimals for the intersection points which can be rounded to the next nearest integer.

3 Summary and conclusion

In this work, we have studied the stability of Z-ply charged (Z=1,2,3,4) metal clusters of species Al, Ga, Li, Na, K, and Cs using the liquid-drop model with stabilized jellium model energies. Fragmentation of clusters into smaller ones can proceed via evaporation or fission. Our results show that, in the LDM, any charged cluster is stable against spontaneous evaporation, and the most favored channel of induced fragmentation depends on the size and the charge of the parent cluster. Sufficiently small multiply charged

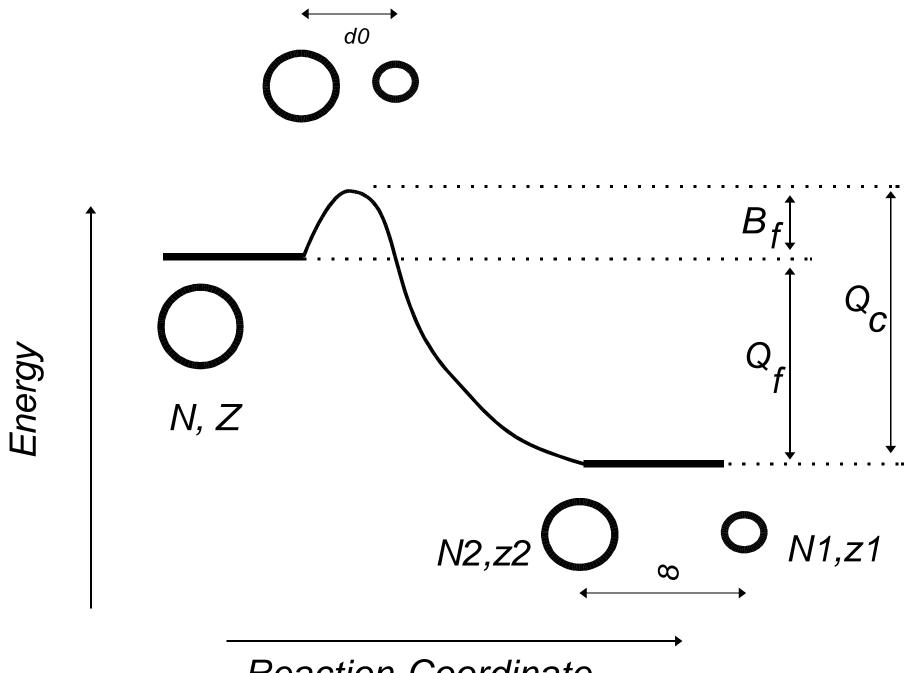
clusters, however, may undergo spontaneous fragmentation via different fission processes. We have obtained, for each species, the smallest size that a Z-ply charged cluster is stable against any spontaneous fragmentation. We have also shown that, for sufficiently large clusters the most favored decay channel is atomic evaporation. Comparing the results for different species show that, for fixed N, the lower electron density clusters have higher capacity for charging. Results also show that, for fixed amount of charge, atomic evaporation dominates at lower Ns for lower electron density metal clusters.

References

- [1] M. Brack, Rev. Mod. Phys. **65**, 677 (1993).
- [2] J. P. Perdew, H. Q. Tran, and E. D. Smith, Phys. Rev. B 42, 11627 (1990).
- [3] U. Näher, S. Bjørnholm, S. Frauendorf, F. Garcias, and C. Guet, Phys. Rep. 285, 245 (1997) and references therein.
- [4] M. Seidl, J. P. Perdew, M. Brajczewska, and C. Fiolhais, Phys. Rev. B 55, 13288 (1997).
- [5] M. Payami, arXiv.org: cond-mat/0212160.
- [6] W. Kohn and L. J. Sham, Phys. Rev. **140**, A1133 (1965).
- [7] M. Payami, J. Phys.: Condens. Matter **13**, 4129 (2001).
- [8] M. Payami, arXiv.org: cond-mat/0305600.

- Figure 1: Fission barrier in the two-spheres approximation. The parent N-atom Z-ply charged cluster decays into two clusters of sizes N_1 and $N N_1$, with charges Z_1 and Z_2 , respectively.
- Figure 2: Coulomb interaction energy of two charged metal spheres, in electron volls, as function of distance. The value of the maximum is B_c , and the location of the maximum is at d_0 . (a)-the spheres have charges 3 and 1, (b)-the spheres have equal charges Z=2, (c)-the charges of the two spheres are exchanged, and (d)-the sizes are kept fixed but the charges are changed.
- Figure 3: Coulomb barrier height, B_c , in electron volts, (a)-for two equally charged but different sized pairs of the same species, (b)-comparison of B_c for different species of equally charged pairs with one of the pair sizes kept fixed.
- Figure 4: Functions of r_s , (a)-total SJM energy per electron in the bulk metal, (b)-the surface energy obtained from fitting to the Kohn-Sham results, and (c)-the curvature energy obtained from fitting.
- Figure 5: Dissociation energy, in electron volts, for different evaporation channels and different parent cluster sizes.(a)-singly ionized, (b)-4-ply ionized Li clusters.
- Figure 6: Na dissociation energy, in electron volts, as function of the parent cluster size, for the most favored channel of different evaporation processes
- Figure 7: Most favored channel dissociation energies, in electron volts, of different species for (a)-singly ionized clusters, (b)-4-ply ionized clusters.
- Figure 8: Fission barrier heights of 4-ply ionized Ga clusters, in electron volts, for different parent sizes and fission channels of (a)-symmetric, (b)-asymmetric processes.
- Figure 9: Barrier energies, in electron volts, in the most favored channel of different sizes of 4-ply ionized Ga clusters. $Z_1 = 1, 2$ correspond to asymmetric and symmetric fission, respectively, while the $Z_1 = 0$ case correspond to evaporation process.
- Figure 10: Most favored fission barrier heights, in electron volts, of different species for (a)- 3-ply ionized, and (b)-doubly ionized clusters.

Figure 11: Functions of r_s , (a)-the minimum stable size for different charges, (b)-the sizes at which evaporation dominates fission, and (c)-the sizes at which the symmetric and asymmetric fissions start their competitions.



Reaction Coordinate

